National Co-ordinating Centre for the Physics of Mammography

Technical evaluation of contrast enhanced mammography functions using Hologic I-View software

Technical Report 2003

November 2020

Mary Kelly, Mandeep Rai, Alistair Mackenzie

Acknowledgements

The authors are grateful to the staff at St Bernard's Hospital and Frimley Park Hospital, as well as Najim Amallal (Service Product Manager and Engineer for Emsor/Hologic) for their assistance with the evaluation of this equipment.

We also acknowledge the use of the contrast enhanced mammography (CEM) phantom from Prof Homolka, Vienna.

Funding

This study was funded for the NHS Breast Screening Programme by Public Health England.

Contents

1. Introduction

1.1 Evaluation report

At the time of publication of this report, contrast enhanced mammography (CEM) systems are not approved for use in the NHS Breast Screening Programme (NHSBSP). The technology is currently being evaluated clinically. Further updates on approvals can be found on the PHE website: https://www.gov.uk/government/publications/breast-screening-status-of-approved-equipment.

This report is one of a series evaluating the use of CEM on commercially available mammography systems and comprises a summary of the performance of CEM. There is currently no NHSBSP guidance on quality control testing of CEM systems. The methodology developed for this evaluation was primarily derived from two publications by Oduko et al.[1,2]

1.2 Objectives

The purpose of the evaluation was to assess the performance of the Hologic I-View software for CEM using the Hologic 3Dimensions and Hologic Selenia Dimensions full field digital mammography systems. Technical evaluations of these systems in 2D modes have previously been carried out.[3,4]

1.3 Contrast enhanced mammography description

CEM involves the administration of an iodinated contrast agent followed by the acquisition of two images in close succession; the first at a low energy and the second at a higher energy. These exposures are designed such that the majority of X-ray energies in the spectra are either below or above the K-edge of iodine. An algorithm is then applied to create an image without breast structure that shows the location of any iodine accumulation. Such accumulation is a potential indicator of cancer.

2. Methods

The following describes the method for testing CEM functions. Any system specific testing methods will be described in the results.

2.1 System tested

Testing was performed on a new Hologic 3Dimensions system installed at St Bernard's Hospital, Gibraltar with some additional confirmatory measurements undertaken on a Hologic Selenia Dimensions system installed in 2017 at Frimley Park Hospital in the UK. Both systems had the same version of software and produced very similar results. Details of the equipment are given in Tables 1 and 2.

Table 1. System 1 description

Location	St Bernard's Hospital, Gibraltar
Manufacturer	Hologic
Model	3Dimensions
Supplier	Emsor S.A.
System Serial Number	3DM160700305
X-ray Tube	Varex Imaging M-113T
Anode target material	Tungsten
Additional filtration	0.05 mm Rhodium (Rh), 0.70 mm Aluminium (Al), 0.05 mm Silver (Ag), 0.3 mm Copper (Cu)
Detector type	Amorphous selenium
Detector model	FFDM-SD
Detector size	Active imaging area not less than 233 mm x 285 mm
Pixel pitch	70 µm
Detector serial number	YB801574
Software version	1.9.1.8

Table 2. System 2 description

Location	Frimley Park Hospital, UK
Manufacturer	Hologic

Model	Selenia Dimensions
Supplier	Hologic
System Serial Number	81009167290
X-ray Tube	Varian M-113T
Anode target material	Tungsten
Additional filtration	0.05 mm Rhodium (Rh), 0.70 mm Aluminium (Al), 0.05 mm Silver (Ag), 0.3 mm Copper (Cu)
Detector type	Amorphous selenium
Detector model	FFDM-SD
Detector size	Active imaging area not less than 233 mm x 285 mm
Pixel pitch	70 µm
Detector serial number	YM865052
Software version	1.9.0.632

All results given are for System 1 unless specified otherwise.

2.2 Phantoms

CEM phantom

A phantom designed by Leithner et al[5] was used in the evaluation. The phantom consists of a 300 x 240 x 20 mm^3 PMMA block. Embedded within the phantom are 5 mm diameter discs containing Iopamidol at concentrations ranging from 0.25 to 2 mg cm^{-2} of iodine. Discs containing 0 mg cm^2 iodine are also included in the phantom, as well as air-filled discs. Figure 1 shows an example subtracted image of the central region of the phantom whilst Figure 2 shows the composition of each disc within the matrix of 8 columns and 5 rows.

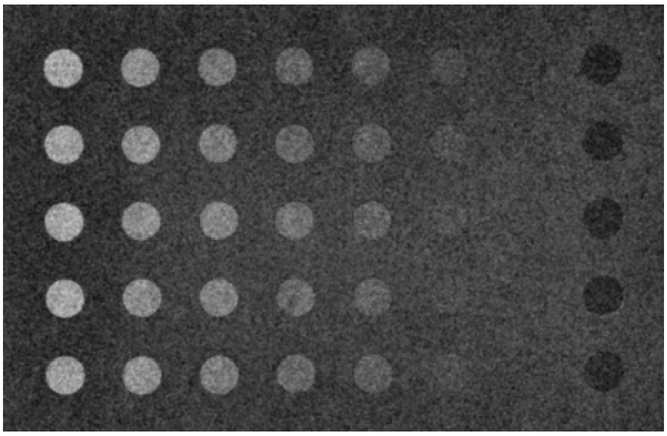

Figure 1. Central region of subtracted image of CEM phantom

2	1.5	1	0.75	0.5	0.25	0	Air
2	1.5	1	0.75	0.5	0.25	0	Air
2	1.5	1	0.75	0.5	0.25	0	Air
2	1.5	1	0.75	0.5	0.25	0	Air
2	1.5	1	0.75	0.5	0.25	0	Air

Figure 2. Iodine concentration of each disc in CEM phantom in terms of mg cm^{-2}. Discs in final column comprised of air.

Tissue equivalent blocks

The majority of the tests were undertaken using tissue equivalent blocks produced by CIRS (Norfolk, VA, USA). These blocks are designed to have similar attenuation properties as for specific fibroglandular densities of breast tissue. Dance *et al*[6] described a model to be used in breast dosimetry for a range of thicknesses from 20 to 110 mm. The model includes two 5 mm thick layers of fat at the upper and lower surface of the breast as well as an expected glandularity for the central portion of the breast. CIRS blocks of different densities by mass were selected to match as closely as possible those densities, in addition to the use of 5 mm of CIRS fat blocks at the bottom and top of the stack. Tables 3 and 4 show the combinations of blocks used to simulate the different breast thicknesses with and without the CEM phantom. Overall, a good match in density was found between the required glandularities and the actual values.

Table 3. CIRS tissue equivalent material used for different phantom thicknesses in addition to two 5 mm thick fat blocks

Total phantom thickness (mm)	Target glandularity of central area (%)	Glandularity of central portion (%)	CIRS Phantom [percentage glandularity] thickness (mm)				
			Fat [0%]	30:70 [30%]	50:50 [50%]	70:30 [70%]	Glandular [100%]
20	100	100					10
30	72	70				20	
40	50	50			30		
50	33	33	10	20		10	
60	21	21	30	10		10	
70	12	12	50			10	
80	7	7	60		10		
90	4	4	70	10			

Table 4. CIRS tissue equivalent material used for different phantom thicknesses in addition to CEM phantom

Total phantom thickness (mm)	Target glandularity of central area (%)	Glandularity of central portion (%)	CIRS Phantom [percentage glandularity] thickness (mm)				
			Fat [0%]	30:70 [30%]	50:50 [50%]	70:30 [70%]	Glandular [100%]
30	72	76			10		
40	50	52	10		10		
50	33	34	20	10			
60	21	22	40				
70	12	18	50				

2.3 X-ray tube output and half value layer

The X-ray tube output and half-value-layer (HVL) were measured as described in the IPEM protocol,[7] at intervals of 3 kV or, if only a limited number of options are used clinically, then only those options were measured.

2.4 Detector performance

Testing was carried out using 50 mm thick tissue equivalent material (Table 3) at the X-ray tube port and with the anti-scatter grid in position. The mean pixel value (PV) and standard deviation were measured in a region of interest. The relationships between mean PV and mAs, as well as variance and mAs, were then determined.

2.5 Uniformity and artefacts

Percentage non-uniformity was measured using an unprocessed high energy image of the CEM phantom and following the methodology described in NHSBSP guidance.[8] Artefact evaluation was performed on low and high energy images. Additional CIRS tissue equivalent material was added in order to evaluate artefacts for subtracted images. Images were viewed using a narrow window to examine any artefacts that may adversely affect clinical image quality.

2.6 Automatic exposure control repeatability

The CEM phantom was imaged with 30 mm thick breast equivalent tissue blocks (Table 4) to achieve a total thickness of 50 mm. The phantom was imaged under automatic exposure control (AEC). This was repeated until three sets of images were acquired.

Subtracted images were analysed to calculate the Signal Difference (SD), i.e. the difference in pixel value between each iodine disc and the background region. The contrast-to-noise ratio (CNR) for each disc was calculated by dividing the SD by the root mean square of the standard deviation in the iodine disc and background region. The SDs and CNRs quoted in this report are the mean values for the five identical discs of each iodine concentration.

In addition to the standard “CEDM” mode, the system has a “CEDM Combo” mode, which acquires both CEM and tomosynthesis images under the same compression. Exposures were performed in CEDM Combo and stand-alone CEDM/ tomosynthesis modes to assess the variation in post-exposure mAs values. For these exposures, a 50 mm thick phantom comprised of only breast equivalent tissue blocks (Table 3) was used.

2.7 Variation in AEC performance and image quality with phantom thickness

The CEM phantom was imaged under AEC with varying combinations of tissue equivalent blocks, as shown in Table 4. Images were analysed to determine the SD and CNR for each iodine concentration.

2.8 Mean glandular dose

Exposures were carried out under AEC using the combinations of tissue equivalent blocks specified in Table 3. The exposure factors were noted and mean glandular doses (MGDs) were calculated for equivalent breast thicknesses using standard methods by Dance et al.[6,9]

The MGD indicated by the system was taken from the DICOM header for both exposures and compared with the calculated value.

2.9 Variation in image quality and MGD between low energy CEM and standard 2D images

Images were acquired of the tissue equivalent blocks listed in Table 3 in standard 2D mode using AEC. MGDs were compared with those calculated for low energy CEM exposures.

Testing was also carried out using a CDMAM phantom (v 3.4) in both CEM and standard 2D mode in order to compare image quality in terms of threshold contrast detail detection. Sixteen images were acquired in AEC mode. CNRs were also measured in both modes in line with the methodology described in the NHSBSP protocol.[8]

CNRs were also measured in both modes by imaging varying thicknesses of 24 cm x 30 cm blocks of PMMA with a 10 mm x 10 mm square, 0.2 mm thick piece of 99.9% purity aluminium. For each thickness of PMMA, an appropriate air gap was used to give a Compressed Breast Thickness (CBT) equal to the equivalent breast thickness.

2.10 Subtraction of BR3D tissue equivalent material

A small sample of iodine was imaged with the tissue-equivalent, heterogeneous material (CIRS BR3D phantom slabs, **Figure 3**) assess whether the system could successfully subtract the tissue-like structures to reveal the iodine sample.

Figure 3. CIRS BR3D phantom

3. Results

3.1 X-ray tube output and half value layer

The X-ray tube output and HVL measurements for the system in high energy mode are shown in Table 5. Measurements were performed with the compression paddle in the X-ray beam.

Table 5. X-ray tube standard output and HVL measurements for high energy CEM image exposure parameters

kV, Target/Filter	Tube Output (μGy/mAs @ 100 cm)	HVL (mm aluminium)
45 kV, W/Cu	2.42	3.16
49 kV, W/Cu	3.71	3.55

Manual exposures using only the W/Cu target/filter combination cannot be carried out in clinical mode; the exposures are always comprised of the low energy exposure (using either the W/Rh or W/Ag target/filter combination) followed by the high energy exposure using the W/Cu combination. A quality control mode is available under the "Admin" option, which enables manual exposures to be carried out using any kV, target, filter combination. Images are not produced in this mode of operation. A lead sheet was used to cover the detector in order to avoid leaving a residual image of any dose meter.

Manual exposures can be carried out in clinical mode; however, a particular set-up resulted in a software error on both systems. The detector was covered with lead, a 24 cm x 30 cm compression paddle was inserted and the CBT set to 53 mm (i.e. no compression). A "PMMA 4.5 cm CEDM" view was added and a manual exposure carried out using 29 kV, Ag filter, 40 mAs, anti-scatter grid in and LFS (large focal spot). For both systems an error message was displayed and the software exited to the login screen.

Hologic provided the following response:
On a 1.9 system

- With lead and manual techniques, the system will display an error message and will exit the application for PMMA CEDM and Patient CEDM Views
- With lead and manual techniques, the "Flat-field CEDM" View (towards the right side of the QC view page) did not give any error
- We did not see any errors with a 4 cm block of acrylic covering the full FOV for any of the views

On a 2.1 (1.10) system

- No errors with lead and manual techniques for any CEDM views (includes both patient and QC views)
- No errors with acrylic for any CEDM views

3.2 Detector performance

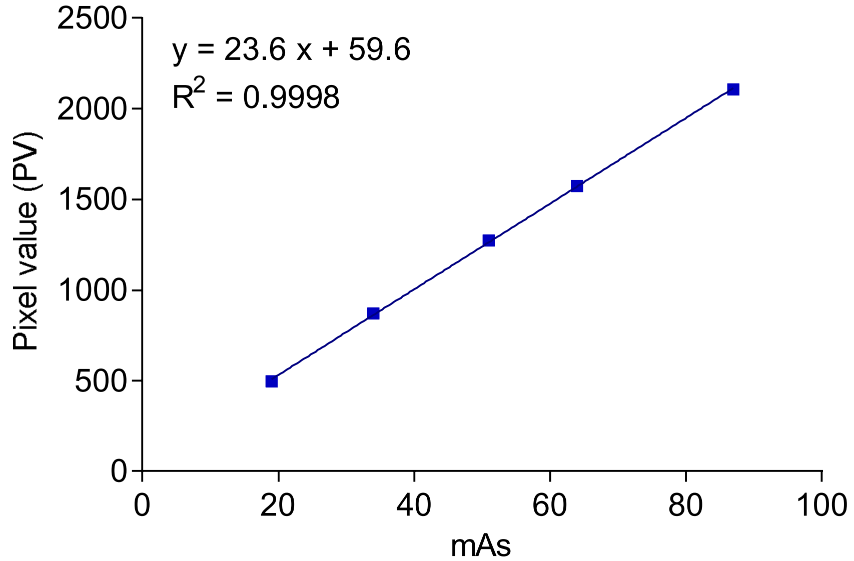

Figure 4. Variation in pixel value of high energy CEM image with mAs

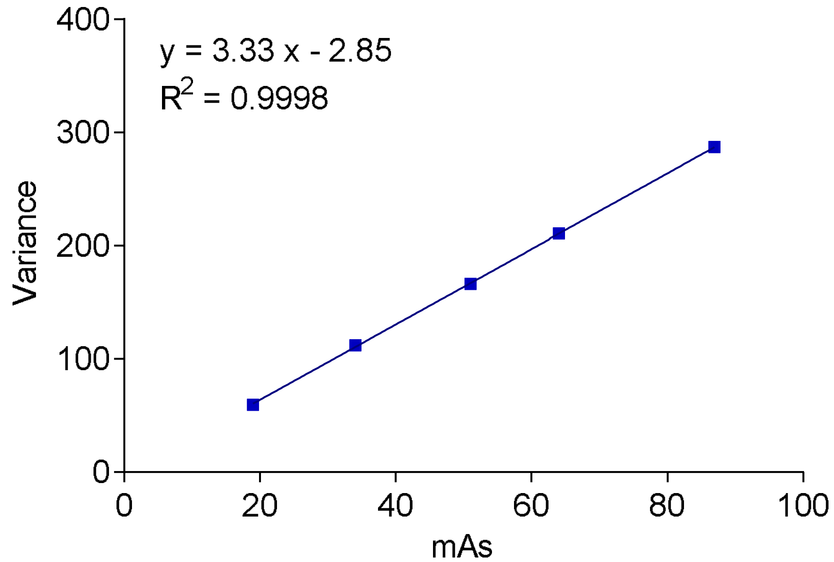

Figure 5. Variation in high energy CEM image variance with mAs

The exposures were acquired using 49 kV and a W/Cu target/filter combination. The representative pixel value (Rep PV) for a raw high energy image acquired of same phantom in Auto-Filter AEC mode was 1178. For phantom thicknesses between 20 and 90 mm, pixel values ranged from approximately 900 to 1500. Figures 4 and 5 demonstrate that pixel value and variance (standard deviation squared) are linear with mAs (and hence detector dose) over this range. The noise (standard deviation) and signal-to-noise (SNR) ratio at the Rep PV were 12.4 and 94.8 respectively.

3.3 Uniformity and artefacts

Percentage non-uniformity was measured for the unprocessed high energy image of the CEM phantom. The maximum variation in pixel value from the centre of the image was 2.4%, which is below the NHSBSP remedial level of 10%.

Artefact evaluation was performed on low and high energy images as well as subtracted images. No artefacts were seen.

It was noted that when a largely uniform phantom (e.g. CIRS consistency testing slab) was positioned at the X-ray tube port and a manual exposure was carried out using the 4.5 cm CEDM view, the resulting subtracted image was blank. This was also the case when imaging the CEM phantom without additional CIRS material or the Hologic flat field phantom (both positioned on the breast support platform). The low and high energy images were however available. Additional CIRS tissue equivalent material was added to the CEM phantom in order to evaluate artefacts for subtracted images.

> Manufacturer comment: For Selenia Dimensions running 1.9 and 3Dimensions running 2.0, it is recommended that the physicist use the "Flat-field CEDM" View to get unprocessed images with the Cu filter for artifact evaluation. However, this view may only provide the Cu filter image on the display.

3.4 Automatic exposure control repeatability

Results for mAs, SD and CNR repeatability under "Auto-Filter" AEC are shown in Table 6. The mAs repeatability was within the NHSBSP recommended remedial tolerance of 5%. Table 7 shows the variation in mAs between CEDM Combo and stand-alone CEDM and tomosynthesis modes.

Table 6. Repeatability of mAs, SD and CNR for CEM exposures

Max variation from mean mAs	Low energy CEM exposure	0%
	High energy CEM exposure	1.5%
Max % variation from mean SD for 1.0 mg cm^{-2} disc		2.4%
Max % variation from mean CNR for 1.0 mg cm^{-2} disc		2.8%

Table 7. Variation in mAs between CEDM Combo and stand-alone CEDM/tomosynthesis exposures

Variation from mean mAs	Low energy exposure	1.4%
	High energy exposure	2.2%
	Tomo exposure	0.0%

3.5 Variation in AEC performance and image quality with phantom thickness

The SD and CNR results for 1.0 mg cm^{-2} iodine for images acquired under "Auto-Filter" AEC are shown in Table 8 with results for other concentrations shown in Figures 5 and 6. For all iodine concentrations, the SD tends to decrease with increasing phantom thickness when imaged in AEC mode (Figure 5); however the CNR remains relatively constant (Figure 6). The SD and CNR increase linearly with iodine concentration for any given phantom thickness (Figures 7 and 8).

Table 8. Variation in exposure parameters, SD and CNR for CEM subtracted images acquired in AEC mode for 1.0 mg cm^{-2}

Phantom thickness (mm)	kV Target/Filter		SD	CNR
	Low energy exposure	High energy exposure		
30	26kV, W/Rh	45kV, W/Cu	62.5	6.1
40	28kV, W/Rh	45kV, W/Cu	57.2	6.2
50	29kV, W/Ag	49kV, W/Cu	50.6	6.3
60	31kV, W/Ag	49kV, W/Cu	47.4	6.7
70	31kV, W/Ag	49kV, W/Cu	47.6	6.9

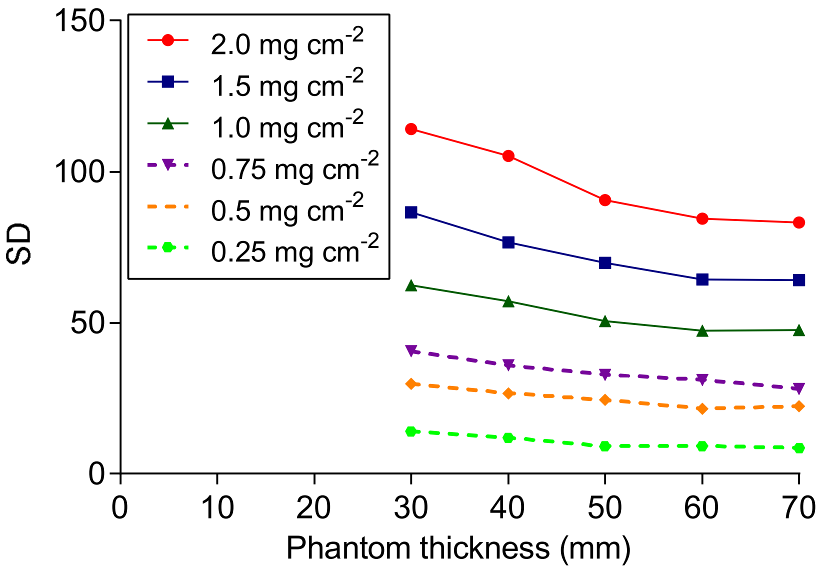

Figure 6. SD with varying phantom thickness for different concentrations of iodine (mg cm^{-2})

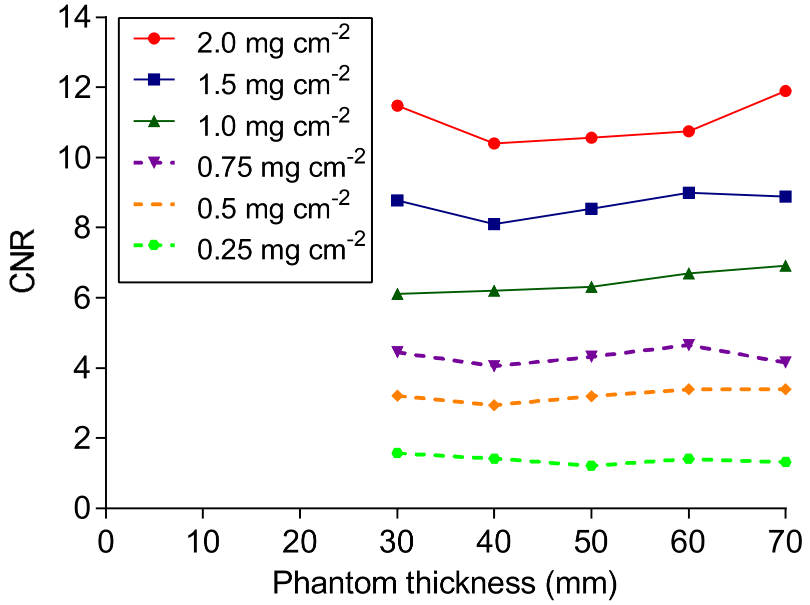

Figure 7. CNR with varying phantom thickness for different concentrations of iodine (mg cm^{-2})

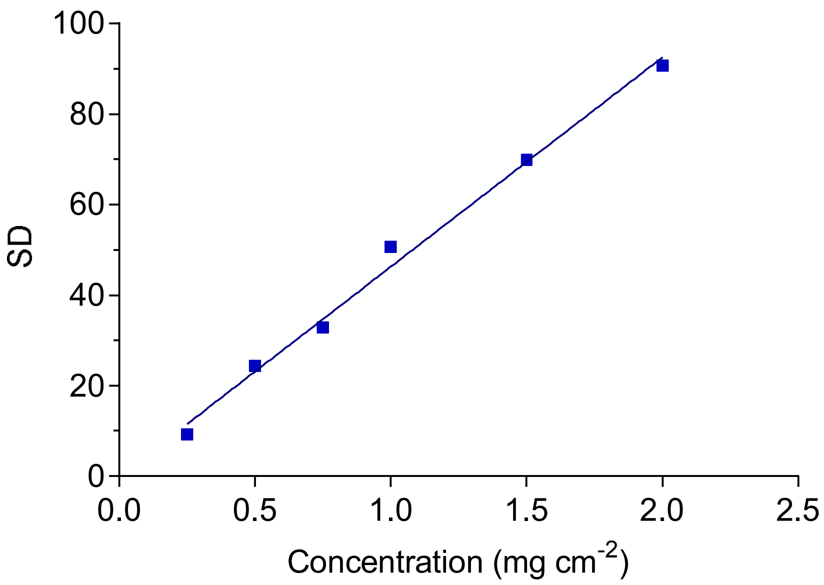

Figure 8. SD with varying iodine concentration for 50 mm thick phantom

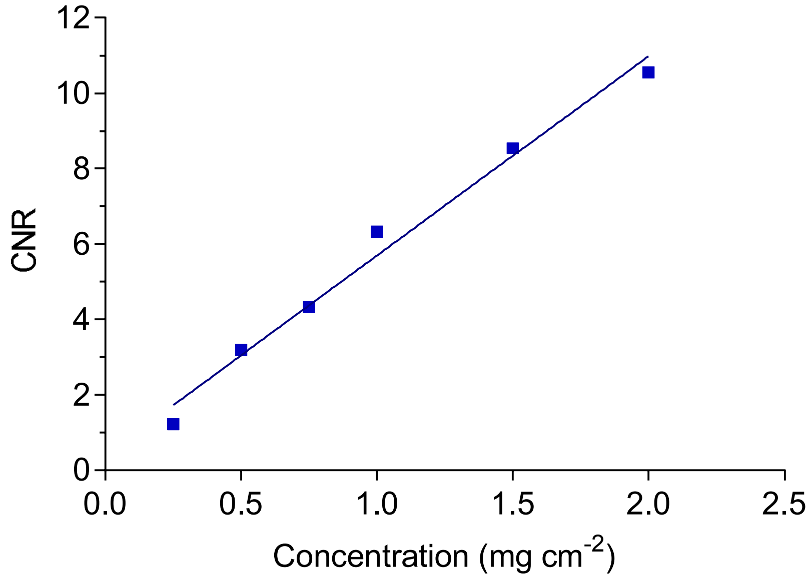

Figure 9. CNR with varying iodine concentration for 50 mm thick phantom

3.6. Mean glandular dose

The MGDs for the tissue equivalent blocks with and without the CEM phantom acquired under "Auto-Filter" AEC are shown in tables 9 and 10 respectively. The value of *s* used in the calculation of MGD for the W/Cu target filter combination was 1.0.

Table 9. MGDs for exposures carried out using CEM phantom with additional tissue equivalent material

Phantom thickness (mm)	Glandularity (%)	Exposure parameters (kV Target/Filter)		Calculated MGD (mGy)		
		Low energy exposure	High energy exposure	Low energy exposure	High energy exposure	Total
30	76	26 W Rh 62 mAs	45 W Cu 46 mAs	0.81	0.28	1.10
40	52	28 W Rh 68 mAs	45 W Cu 54 mAs	0.96	0.32	1.28
50	34	29 W Ag 75 mAs	49 W Cu 46 mAs	1.26	0.43	1.69
60	22	31 W Ag 98 mAs	49 W Cu 68 mAs	1.85	0.61	2.46
70	18	31 W Ag 138 mAs	49 W Cu 89 mAs	2.42	0.78	3.20

Table 10. MGDs for exposures carried out using tissue equivalent material only

Phantom thickness (mm)	Glandularity (%)	Exposure parameters (kV Target/Filter)		Calculated MGD (mGy)		
		Low energy exposure	High energy exposure	Low energy exposure	High energy exposure	Total
20	100	26 W Rh 35 mAs	45 W Cu 32 mAs	0.59	0.21	0.79
30	70	26 W Rh 60 mAs	45 W Cu 44 mAs	0.79	0.27	1.06
40	50	28 W Rh 66 mAs	45 W Cu 52 mAs	0.93	0.31	1.24
50	33	29 W Ag 73 mAs	49 W Cu 44 mAs	1.23	0.41	1.64
60	21	31 W Ag 95 mAs	49 W Cu 66 mAs	1.79	0.60	2.39
70	12	31 W Ag 129 mAs	49 W Cu 84 mAs	2.26	0.73	3.00
80	7	32 W Ag 140 mAs	49 W Cu 96 mAs	2.50	0.81	3.31
90	4	33 W Ag 146 mAs	49 W Cu 102 mAs	2.67	0.83	3.50

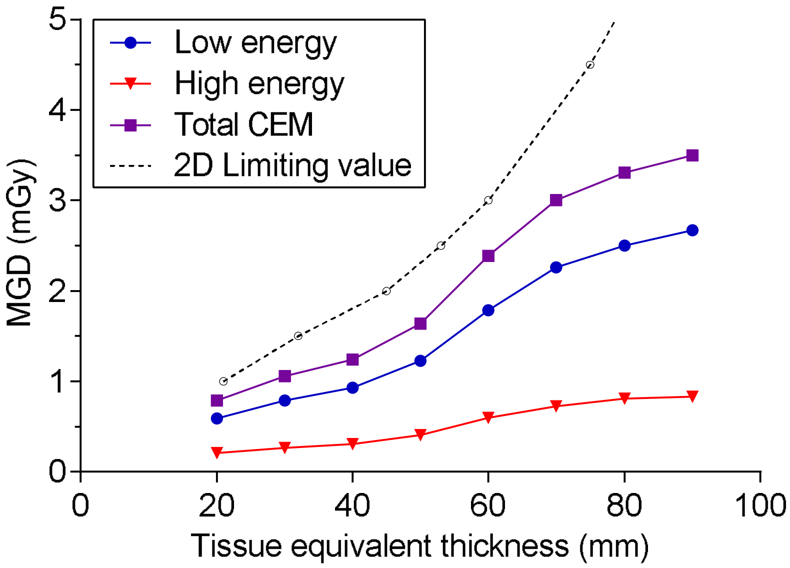

Figure 10. MGD for tissue equivalent material

The MGDs for tissue equivalent material are shown in Figure 10. CEM is a different imaging modality from standard 2D imaging and so the limiting dose values are not relevant, but it is of interest to compare them. It can be seen that the calculated total MGDs are below the limiting dose values for 2D screening for all phantom thicknesses.

MGDs calculated for phantoms comprised of only tissue equivalent material were well matched to those calculated for the CIRS phantom with additional tissue equivalent material. This demonstrates that the percentage glandularities of the phantoms were reasonably comparable.

The relationship between MGD and phantom thickness appears to be sigmoid, as shown in Figure 10. The ratio of MGDs for low and high energy exposures is approximately three.

3.7. Accuracy of indicated MGD

Table 11. Accuracy of indicated MGD

Phantom thickness (mm)	MGD (mGy) for low energy exposure			MGD (mGy) for high energy exposure			Difference for total MGD
	Calculated	Indicated	Difference	Calculated	Indicated	Difference	
20	0.59	0.61	4.2%	0.21	0.21	2.4%	3.8%
30	0.79	0.80	1.8%	0.27	0.27	-0.9%	1.1%
40	0.93	0.96	3.6%	0.31	0.31	-0.6%	2.5%
50	1.23	1.27	3.4%	0.41	0.40	-2.6%	1.9%
60	1.79	1.89	5.4%	0.60	0.58	-2.8%	3.4%
70	2.26	2.40	6.1%	0.73	0.72	-2.0%	4.1%
80	2.50	2.71	8.2%	0.81	0.79	-2.5%	5.6%
90	2.67	2.93	9.9%	0.83	0.82	-1.3%	7.3%

Table 11 shows the difference between the calculated MGDs and the MGDs shown by the system for tissue equivalent material only. The maximum difference between the indicated and calculated MGDs was 9.9% for the low energy exposure, 2.8% for the high energy exposure and 7.3% for the total MGD.

3.8 Variation in image quality and MGD between low energy CEM and standard 2D images

Exposure parameters (kV and filter) vary slightly between low energy CEM exposures and standard 2D exposures, as shown in Table 12, due to the use of a different lookup table. The default is Hologic Table 4 for standard 2D exposures and Hologic Table 0 for CEM low energy exposures. Hologic have provided feedback on the reasons for the differences in exposure techniques as follows:

- For the very thin breasts, phantom subtracted imaging is slightly superior when the kV is increased from 25 kV to 26 kV.
- For the largest breasts (≥ 90 mm), the kV is not increased above 33 kV to avoid exceeding the k-edge of iodine.
- For breast thicknesses between 50 mm and 65 mm, the filter has been changed from Rh to Ag to increase the flux per tube mAs, allowing identical MGDs to 2D mode but with reduced tube loading. This range of breast thicknesses is the most common and therefore it was considered important to reduce tube loading in this region.

Table 12. Variation in MGD for low energy CEM and standard 2D exposures carried out in "Auto-Filter" AEC mode (System 2) using tissue equivalent material only

Phantom thickness (mm)	Low energy CEM exposure		Standard 2D exposure		Difference between MGDs
	Exposure parameters (kV Target/Filter)	MGD (mGy)	Exposure parameters (kV Target/Filter)	MGD (mGy)	
20	26 W Rh	0.56	25 W Rh	0.56	0.8%
30	26 W Rh	0.74	26 W Rh	0.72	-2.5%
40	28 W Rh	0.92	28 W Rh	0.89	-3.3%
50	29 W Ag	1.20	29 W Rh	1.20	0.3%
60	31 W Ag	1.85	31 W Rh	1.81	-2.0%
70	31 W Ag	2.35	30 W Ag	2.23	-5.4%
80	32 W Ag	2.71	32 W Ag	2.72	0.5%
90	33 W Ag	2.94	34 W Ag	3.05	4.0%

It is understood from Hologic that low energy CEM images can be used in place of the standard 2D images for reporting purposes. Image quality testing of low energy CEM and standard 2D images acquired using System 2 was carried out according to the methodology described in NHSBSP Report 0604. This included CDMAM and CNR measurements.

A CDMAM phantom was imaged in both CEM and standard 2D modes and threshold gold thicknesses for different detail diameters were compared as shown in Figure 11. Negligible differences were seen between the two exposure modes and all results met the achievable level of image quality expected for modern full field digital mammography systems.

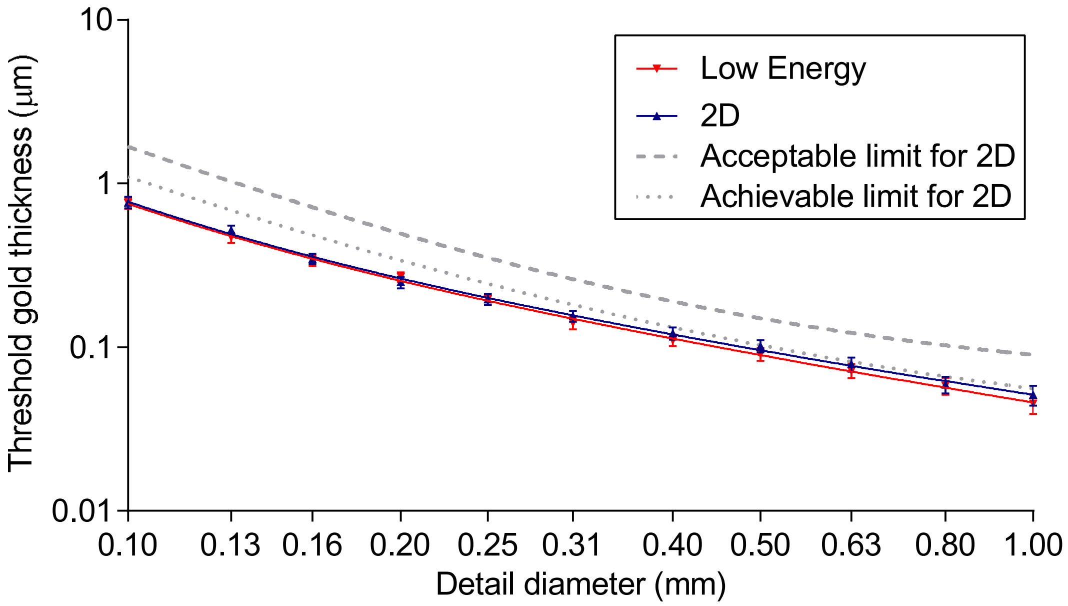

Figure 11. Threshold gold thicknesses for varying detail diameters measured using a CDMAM phantom for low energy CEM and standard 2D images. Error bars show ±2 standard errors of the mean

CNR measurements for low energy CEM and standard 2D images are summarised in Table 13. The maximum variation in CNR was -4.0%.

Table 13. Variation in CNR for low energy CEM and standard 2D exposures carried out in "Auto-Filter" AEC mode (System 2)

PMMA thickness (mm)	Equivalent breast thickness (mm)	CNR		Difference between CNRs
		Low energy CEM image	Standard 2D image	
20	21	8.80	9.16	-4.0%
30	32	8.33	8.06	3.3%
40	45	7.48	7.54	-0.8%
45	53	7.15	7.17	-0.3%
50	60	7.42	7.34	1.1%
60	75	6.86	6.88	-0.3%
70	90	5.66	5.72	-1.0%

3.9 Subtraction of BR3D tissue equivalent material

Figure 12 demonstrates the successful subtraction of the tissue-like structures in the CIRS BR3D phantom (Figure 11) to reveal the iodine sample.

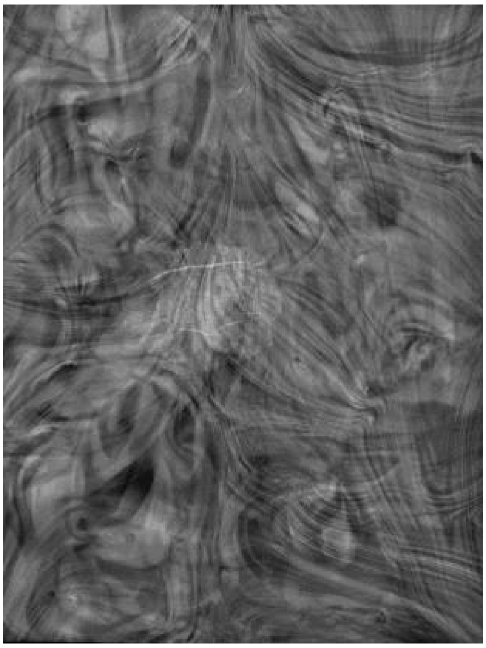

Figure 12. Low energy image of iodine sample with BR3D material

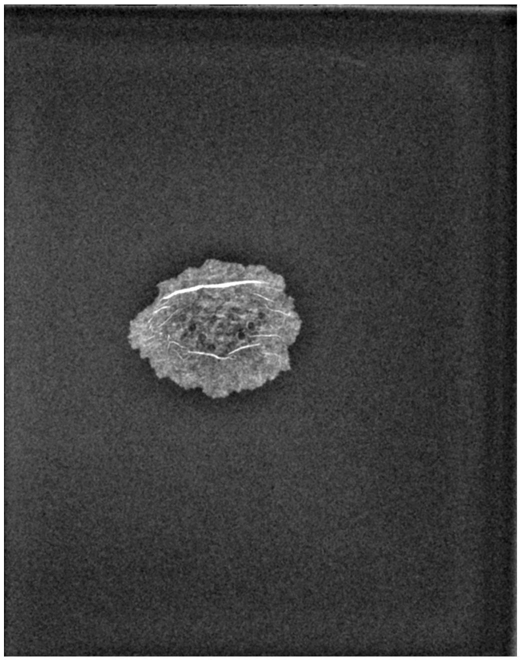

Figure 13. Subtracted image of iodine sample with BR3D material

4. Discussion

4.1 Detector response, uniformity and artefacts

- Image pixel value and variance are linear with mAs (and hence detector dose) over the typical clinical pixel value range.
- Percentage non-uniformity measured using an unprocessed high energy image of the CEM phantom was 2.4%. No artefacts were seen on low and high energy images or subtracted images.

4.2 Automatic exposure control

- Exposures in “Auto-Filter” AEC mode are repeatable in terms of mAs, SD and CNR. Post exposure mAs values are consistent for CEDM Combo and stand-alone CEDM/ Tomosynthesis modes.
- Exposure parameters (kV and filter) vary slightly between low energy CEM exposures and standard 2D exposures due to the use of a different lookup table. It is understood from Hologic that the low energy CEM images can be used in place of the standard 2D images for reporting purposes. There is a negligible difference in image quality and MGD between the two exposure modes.

4.3 Mean glandular dose

- The MGD for the 50 mm thick tissue equivalent phantom was 1.23 mGy and 0.41 mGy for the low and high energy contrast imaging exposures respectively.
- The total MGD for a CEM exposure is approximately 1.33 times the MGD from the low energy exposure alone. All MGDs are below the dose limiting values for 2D screening mammography.
- The maximum deviation between the indicated and calculated MGD was 9.9% for the low energy CEM exposure and 2.8% for the high energy CEM exposure, with a maximum error of 7.3% for the total MGD.

4.4 Image quality

- For all iodine concentrations, the SD decreases with increasing phantom thickness when imaged in “Auto-Filter” AEC mode; however the CNR remains relatively constant. The SD and CNR increase linearly with iodine concentration for any given phantom thickness.

4.5 Image subtraction

- When the CEM phantom is imaged without any additional CIRS material, a blank subtracted image is produced. It is understood from Hologic that this is expected when imaging non-tissue equivalent material and will not affect clinical use.

- When an exposure is carried out of a uniform phantom covering the full detector the resulting subtracted image is blank. This is understood from Hologic to be expected when imaging a uniform test phantom. The low and high energy images are however available for artefact analysis.

- The system was able to successfully subtract the tissue-like structures in the BR3D material to reveal the iodine sample imaged.

5. Conclusions

The system was found to be operating satisfactorily. Variations in SD and CNR with iodine concentration and phantom thickness follow similar trends to those seen in published data.[1,2]

References:

1. Oduko, J., Homolka, P., Jones, V. and Whitwam, D. A Protocol for Quality Control Testing for Contrast-Enhanced Dual Energy Mammography Systems. In: Fujita H., Hara T. and Muramatsu C. eds. *IWDM 2014: Breast Imaging, 29 June – 2 July 2014,* Gifu City, Japan. Switzerland: Lecture Notes in Computer Science, Springer, Cham. 8539, pp. 407-414.

2. Oduko, J., Homolka, P., Jones, V. and Whitwam, D. Dose and Image Quality Measurements for Contrast-Enhanced Dual Energy Mammography Systems. Proceedings of SPIE, Medical Imaging 2015: Physics of Medical Imaging. Proceedings of SPIE. 2015, 9412, 94125I-1.

3. Mackenzie A, Oduko JM. NHSBSP Equipment Report. Technical evaluation of Hologic 3Dimensions digital mammography system in 2D mode. London: Public Health England, 2019

4. Young KC, Oduko JM. *Technical evaluation of Hologic Selenia Dimensions 2-D Digital Breast Imaging System with software version 1.4.2* (NHSBSP Equipment Report 1201). Sheffield: NHS Cancer Screening Programmes, 2012

5. Leithner R, Knogler T, Homolka P. Development and production of a prototype iodine contrast phantom for CEDEM, Physics in Medicine and Biology, 2013, 58, N25-35,

6. Dance, D.R., Skinner, C.L., Young, K.C., Beckett, J.R. and Kotre, C.J. Additional factors for the estimation of mean glandular breast dose using the UK mammography dosimetry protocol. Physics in Medicine and Biology. 2000, 45, pp. 3225–3240.

7. Moore AC, Dance DR, Evans DS et al. The Commissioning and Routine Testing of Mammographic X-ray Systems. York: Institute of Physics and Engineering in Medicine, Report 89, 2005

8. Kulama E, Burch A, Castellano I et al. *Commissioning and routine testing of full field digital mammography systems* (NHSBSP Equipment Report 0604, Version 3). Sheffield: NHS Cancer Screening Programmes, 2009

9. Dance, D.R. and Young, K.C. Estimation of mean glandular dose for contrast enhanced mammography: factors for use with the UK, European and IAEA breast dosimetry protocols. Physics in Medicine and Biology. 2014, 59, pp. 2127–2137.